Density wave and topological reconstruction of an isotropic two-dimensional electron band in external magnetic field

Kadigrobov, Anatoly M.; Radić, Danko; Bjeliš, Aleksa

Source / Izvornik: **Physical Review B, 2019, 100**

Journal article, Published version
Rad u časopisu, Objavljena verzija rada (izdavačev PDF)

https://doi.org/10.1103/PhysRevB.100.115108

Permanent link / Trajna poveznica: https://urn.nsk.hr/urn:nbn:hr:217:602860

Density wave and topological reconstruction of an isotropic two-dimensional electron band in external magnetic field

A. M. Kadigrobov,[1,2,*] D. Radić,[2,†] and A. Bjeliš[2]
[1]*Theoretische Physik III, Ruhr-Universitaet Bochum, D-44801 Bochum, Germany*
[2]*Department of Physics, Faculty of Science, University of Zagreb, 10000 Zagreb, Croatia*

(Received 3 July 2019; published 3 September 2019)

We predict a mechanism of spontaneous stabilization of a uniaxial density wave in a two-dimensional metal with an isotropic Fermi surface in the presence of external magnetic field. The topological transformation of a closed Fermi surface into an open one decreases the electron band energy due to delocalization of electrons initially localized by magnetic field, additionally affected by the magnetic breakdown effect. The driving mechanism of such reconstruction is a periodic potential due to the self-consistently formed electron density wave. It is accompanied with quantum oscillations periodic in inverse magnetic field, similar to the standard de Haas-van Alphen effect, due to Landau-level filling. The phase transition appears as a quantum one at $T = 0$, provided the relevant coupling constant is above the critical one. This critical value rapidly decreases, and finally saturates toward zero on the scale of tens of Tesla. Thus, a strong enough magnetic field can induce the density wave in the system in which it was absent in zero field.

DOI: 10.1103/PhysRevB.100.115108

I. INTRODUCTION

The instability of low-dimensional conductors with the spontaneous arising of a periodic modulation of the crystal, usually called the density wave (DW) [1], remains the focus of attention since its early prediction by Peierls [2] almost 90 years ago. In one-dimensional (1D) conductors, the crystal modulation opens a gap in the electron band at the initial Fermi energy, decreasing the electron band energy. The new DW ordering is stabilized whenever this energy decrease overwhelms the competing increase of the crystal energy caused by the accompanying lattice modulation.

The DW instability also arises in the special class of two-dimensional (2D) systems, often also called quasi-one-dimensional (quasi-1D) systems, with a highly anisotropic, mainly open Fermi surface (FS), such that the parts of its contour can be (almost) perfectly mapped, i.e., nested, onto each other. DWs of this type have been intensively investigated and widely observed in the series of different materials possessing such band dispersions [1,3].

However, DWs have not only been observed in conductors with highly anisotropic FSs, but also in many 2D conductors with closed FSs for which the nesting condition as specified above is far from being fulfilled. Particularly significant in this respect are high-temperature superconducting cuprates with conducting CuO_2 layers [4], as well as hexagonal (semi)metallic layers appearing in graphene-based intercalates, like in, e.g., CaC_6 [5]. Despite intensive investigations of these and similar materials, the origin of the observed structural instability is still a controversial topic.

In our recent paper [6], we proposed a mechanism of the DW ordering based on the topological reconstruction of the highly symmetric, initially closed FS. As shown in Fig. 1(a), the DW has a wave vector $\mathbf{Q}/\hbar$ that brings the initial FS into the so-called touching range generated at the edge of the Brillouin zone established by the DW periodic modulation in the system. By lifting the energy degeneracy and opening the gap in that region, the band topology changes: two parabolic initial bands now form the lower band with the saddle point and the upper band with a parabolic minimum at the touching point [6]. The new FS then becomes open as shown in Fig. 1(b), while the total band energy is decreased. In principle, this decrease may stem from two contributions: lowering of the new Fermi energy with respect to the original one and the change in the DOS due to the redistribution of filled states from higher toward lower energies. It appears that in the particular analyzed case [6], and for the optimal DW wave vector, there is only the contribution that comes from the redistribution of states, while the Fermi energy shows no change.

Let us now focus on the role that the external magnetic field may have in the DW ordering and the accompanying band reconstruction. Namely, as has been observed in various 2D conductors—in particular, in high-temperature cuprates [7–9]—it appears that DWs also spontaneously arise under a strong enough external magnetic field. These magnetic-field-induced DWs have been most often associated to the Landau quantization of orbits in relatively small pockets in the anisotropic bands [10–12]. Within this framework, particularly interesting is the role of magnetic breakdown (MB) due to the tunneling of electrons through the narrow barriers in the reciprocal space, quite often present in the band spectra under question [13,14]. In fact, in a few earlier papers [15,16], we pointed out that the electron delocalization due to such tunneling could itself have the decisive role in the stabilization of the so-called MB-induced density waves.

*kadig@tp3.rub.de
†dradic@phy.hr

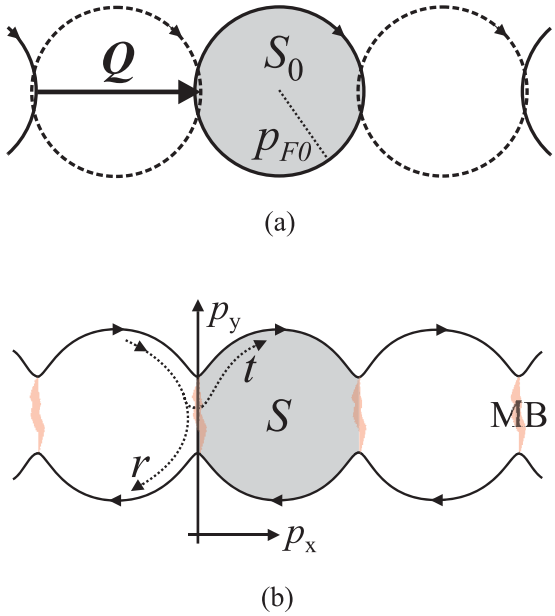

FIG. 1. (a) The reciprocal space for the isotropic 2D band with the Fermi momentum p_{F0} and the DW which introduces the 1D reciprocal lattice with the wave number $Q/\hbar$ close to $2p_{F0}/\hbar$. (b) Two open lines representing the reconstructed FS due to the finite amplitude of the DW in the presence of finite magnetic field directed perpendicularly to the plane (p_x, p_y), enabling finite MB probability amplitudes t and r.

Our prediction was based on the analysis of 2D conductors with open FSs (as is the case of e.g., some compounds from the family of Bechgaard salts) in the presence of strong external magnetic fields [17]. The physical mechanism causing this phase transition is specific with respect to those of the standard Peierls transition in quasi-1D conductors. Namely, under a strong magnetic field, electrons of the 2D conductor with the open FS move in opposite directions along two trajectories defined by the equation $\varepsilon(p) = \varepsilon_F$, where $\varepsilon(p)$ defines the band dispersion, ε_F is Fermi energy, and space inversion is assumed. As suggested in Refs. [15,16], the periodic modulation of electronic charge caused by the DW transforms the open FS into a periodic chain of the overlapping above-mentioned trajectories with lifted band degeneracy in the crossing points of two initially open subbands. As a result, after the band reconstruction, electrons move in the presence of magnetic field along a 1D chain of trajectories with periodically located scatterers—small areas around the crossing points at which the MB [18,19], the quantum tunneling between the neighboring trajectories, takes place. In other words, within the reconstructed FS, electrons under magnetic field move along a 1D periodic set of quantum barriers and hence the system is mapped onto the 1D metal with the "crystal" period of the order of the Larmor radius $R_H = c\overline{p}_F/eH$, where H is the magnetic field, $\overline{p}_F$ is the value of the longitudinal Fermi wave vector averaged over the reciprocal space, e is the electron charge, and c is the velocity of light. The emerging electron spectrum will thus be a set of alternating narrow energy bands and energy gaps. The transition of Peierls type in such a system takes place provided the initial Fermi energy is inside one of the gaps in the new spectrum.

Evidently, since the above physical considerations and results of the cited papers have the quasi-2D band dispersions with open FSs as the starting point, they cannot be straightforwardly transposed to highly isotropic 2D conductors with closed FSs. Still, as stated above, the band reconstruction due to a finite DW introduces here as well as the 1D periodic set of barriers, and the quantum tunneling in the finite magnetic field is again unavoidable. In the present paper, we consider the latter situation. Extending the treatment initiated in our previous paper [6], we show that in such situation one can stabilize the DW under a strong magnetic field as well. Even more, we show that under magnetic field the DW order is additionally strengthened and appears at lower values of the critical coupling constant.

The underlying physical reason for this stabilization is as follows. As already mentioned, the DW causes a topological band reconstruction under which the initially closed 2D FS [Fig. 1(a)] is transformed into an open one [Fig. 1(b)]. Let us now impose the perpendicular magnetic field and consider its effects within the semiclassical reasoning. Without the band reconstruction, electrons would move along initially closed FSs, with the discrete spectrum consisting of degenerate Landau levels and with an increase of the band energy on average. However, having the reconstruction, the semiclassical motion along open trajectories delocalizes band states and decreases their energy. This delocalization itself would therefore act toward an additional stabilization of the DW, besides that realized due to the band reconstruction in the absence of magnetic field.

However, the picture of electron dynamics is not completed by this. As seen in Fig. 1(b), two open trajectories are close to each other in the touching range of the reconstructed band, enabling in this range the MB, i.e., the tunneling of electrons from one open trajectory to another. The finite tunneling is characterized by two probability amplitudes for an electron, t, to pass through the barrier and continue the motion along the same open trajectory, and r to get reflected back and start to move in the opposite direction along the second trajectory, with $t^2 + r^2 = 1$. The MB due to the finiteness of r partially relocalizes the effective electron states and increases the corresponding band energy, thus acting against the DW stabilization.

Aiming to make the quantitative analysis of these two opposite tendencies, we formulate the appropriate mean-field approach and undertake the detailed calculation of the band spectrum and of the corresponding total energy of ground state in the presence of external magnetic field. By this, we arrive at the conditions for the stabilization of the DW and reconstructed band in the magnetic field. In particular, we determine the range of the effective strength of electron-phonon coupling (or of the coupling to some other effective or real boson field), under which the DW ordering takes place in the given magnetic field.

In Sec. II, we start with the electron-phonon Hamiltonian in the presence of finite magnetic field, and introduce the mean-field approximation relevant for the stabilization of DW and band reconstruction. The impact of the magnetic field on the band reconstruction, which includes the semiclassical treatment of uniaxial electron trajectories and the MB in the ranges of topological change of the initial 2D band, is treated in

Sec. III. In Sec. IV, we calculate the total band energy, while in Sec. V the minimization of the total DW condensation energy leads us to the determination of the optimal amplitude, the wave number of the DW order, and their dependence on the magnetic field and the electron-phonon coupling constant. Section VI contains concluding remarks.

II. HAMILTONIAN AND MEAN-FIELD APPROXIMATION

For the sake of simplicity, we consider a 2D conductor with the electron band which initially has a parabolic dispersion $\epsilon_0(k_x, k_y) = (k_x^2 + k_y^2)/2m$, where $\mathbf{k} = (k_x, k_y)$ is the electron momentum and m is the effective electron mass. Taking the Hamiltonian, describing the coupled electron-phonon system in the momentum representation, and making the Peierls substitution with the momentum operator $\hat{\mathbf{k}}$ replaced by the operator $\hat{\mathbf{k}} - (e/c)\mathbf{A}$, where $\mathbf{A}$ is the vector potential, one gets

$$\mathcal{H} = \frac{1}{2m}\sum_{\mathbf{k}} a_{\mathbf{k}}^{\dagger}\left[k_x^2 + \left(k_y + i\frac{e\hbar H}{c}\frac{\partial}{\partial k_x}\right)^2\right]a_{\mathbf{k}} + \sum_{\mathbf{q}}\hbar\omega(\mathbf{q})b_{\mathbf{q}}^{\dagger}b_{\mathbf{q}} + \frac{1}{\sqrt{A}}g\sum_{\mathbf{k},\mathbf{q}} a_{\mathbf{k}+\mathbf{q}}^{\dagger}a_{\mathbf{k}}(b_{-\mathbf{q}}^{\dagger} + b_{\mathbf{q}}). \quad (1)$$

Here we use the Landau gauge for which the vector potential is given by $\mathbf{A} = (0, Hx, 0)$. $a_{\mathbf{k}}^{\dagger}$ and $a_{\mathbf{k}}$ are the creation and annihilation operators for electron states with momentum $\mathbf{k} = (k_x, k_y)$ and energy $\varepsilon_0(\mathbf{k})$, while $b_{\mathbf{q}}^{\dagger}$, $b_{\mathbf{q}}$ are corresponding operators for phonon states with momentum $\mathbf{q} = (q_x, q_y)$ and energy $\hbar\omega(\mathbf{q})$. The electron-phonon coupling constant g is assumed to be independent of $\mathbf{q}$. A is the area of 2D crystal.

Let us now make the first approximation in the treatment of the Hamiltonian Eq. (1). We replace the phonon field by its mean-field value,

$$g(b_{\mathbf{q}} + b_{-\mathbf{q}}^{\dagger}) \to g(\langle b_{\mathbf{q}}\rangle + \langle b_{-\mathbf{q}}^{\dagger}\rangle) = \delta_{\mathbf{q},\mathbf{Q}}\sqrt{\mathrm{A}}\Delta e^{i\Phi}, \quad (2)$$

where the order parameter $\Delta e^{i\Phi}$ is the nonvanishing expectation value of the macroscopically occupied DW phonon mode.

The values of the order parameter amplitude Δ and the modulus of the DW momentum $Q \equiv |\mathbf{Q}|$ will be determined later by the minimization of the total energy of the system. Note that the direction of the wave vector is arbitrary. This degeneracy follows from the assumed spatial isotropy of the band dispersion $\varepsilon_0(\mathbf{k})$, as well as of the phonon spectrum and of the electron-phonon coupling. Φ, the phase of the order parameter, is also arbitrary. The phase degeneracy is present as long as one does not take into account any possible pinning mechanisms, e.g., the commensurability of the DW and the crystal lattice or the effects of various irregularities (like impurities, crystal edges, etc.).

After the mean-field step Eq. (2), the Hamiltonian Eq. (1) reduces to

$$\mathcal{H} = \frac{1}{2m}\sum_{\mathbf{k}} a_{\mathbf{k}}^{\dagger}\left[k_x^2 + \left(k_y + i\frac{e\hbar H}{c}\frac{\partial}{\partial k_x}\right)^2\right]a_{\mathbf{k}} + \sum_{\mathbf{k}}[\Delta e^{i\Phi}a_{\mathbf{k}+\mathbf{Q}}^{\dagger}a_{\mathbf{k}} + \Delta e^{-i\Phi}a_{\mathbf{k}-\mathbf{Q}}^{\dagger}a_{\mathbf{k}}] + \frac{\mathrm{A}\hbar\omega_Q}{2g^2}\Delta^2, \quad (3)$$

where $\omega_Q \equiv \omega(\mathbf{q} = \mathbf{Q})$. The comprehensive analysis of this Hamiltonian,i.e., of the band reconstruction due to the DW order, in the case of vanishing magnetic field ($H = 0$) is given in Ref. [6]. For finite magnetic fields, it is more convenient to diagonalize the Hamiltonian by using the coordinate representation of the electron field:

$$\hat{\Psi}(\mathbf{r}) = \sum_{\mathbf{k}} a_{\mathbf{k}}\exp\{i\mathbf{k}\mathbf{r}/\hbar\}. \quad (4)$$

The Hamiltonian Eq. (3) then reads

$$\mathcal{H} = \frac{1}{2m}\int \hat{\Psi}^{\dagger}(\mathbf{r})\left\{-\hbar^2\frac{\partial^2}{\partial x^2} + \left(-i\hbar\frac{\partial}{\partial y} - \frac{eHx}{c}\right)^2 + 2\Delta\cos(\mathbf{Q}\mathbf{r}/\hbar + \Phi)\right\}\hat{\Psi}(\mathbf{r}) + \frac{\mathrm{A}\hbar\omega_Q}{2g^2}\Delta^2. \quad (5)$$

In the next section, we show how in the presence of both finite DW modulation and finite magnetic field, topological reconstruction of the FS takes place, changing electron dynamics into one of a peculiar MB type.

III. ELECTRON DYNAMICS UNDER MAGNETIC BREAKDOWN CONDITIONS

In this section, we assume strong magnetic fields, characterized by the regime $\omega_0 \ll \omega_H \ll \varepsilon_F/\hbar$, where ω_0 is the electron relaxation frequency and $\omega_H = eH/mc$ is the cyclotron frequency. As one sees from Eq. (5), the electron states are the solutions of the effective one-electron Hamiltonian

$$\mathcal{H}_b = \frac{1}{2m}\left\{-\hbar^2\frac{\partial^2}{\partial x^2} + \left(-i\hbar\frac{\partial}{\partial y} - \frac{eHx}{c}\right)^2\right\} + V(x), \quad (6)$$

where $V(x)$ is the potential associated to the uniaxial DW charge modulation in the x direction:

$$V(x) = 2\Delta\cos(Qx/\hbar). \quad (7)$$

Here the free phase of the DW order parameter is chosen to be $\Phi = 0$.

In the momentum representation, far from small regions were the MB takes place (below we define these regions more precisely), the dynamics of electrons is semiclassical. For further consideration, it is convenient to use, as in Ref. [6], the new origin in the momentum space coinciding with the touching point due to the finite DW, with corresponding electron momentum components $p_x = k_x + Q/2$, $p_y = k_y$, and the first Brillouin zone defined by $-Q/2 \leqslant p_x \leqslant Q/2$ (see Fig. 1 in which these coordinates are already used). Then the Hamiltonian Eq. (6) can be replaced by the Lifshitz-Onsager equation [20,21],

$$\varepsilon\left(p_x \pm Q/2, P_{y0} - i\sigma\frac{d}{dp_x}\right)G(p_x, P_{y0}) = \varepsilon G(p_x, P_{y0}), \quad \varepsilon(p_x \pm Q/2, p_y) = \varepsilon, \quad (8)$$

for wave functions $G(p_x, p_y)$, where $\varepsilon(p_x \pm Q/2, p_y)$ is the band dispersion law of the initial system in the absence of magnetic field ($H = 0$), with its center $p_x = p_y = 0$ in the origin of the coordinate system. Here P_{y0} is the conserved y component of the generalized momentum, $\sigma = \hbar^2/l_c^2 = e\hbar H/c$ is the magnetic area in the momentum space, and $l_c =$

$\sqrt{\hbar c/eH}$ is the magnetic length. The second line in Eqs. (8) is the energy conservation law that defines the semiclassical electron trajectories in the momentum space shown in Fig. 1.

The solution of Eqs. (8) must satisfy the periodic boundary condition $G(p_x, P_{y0}) = G(p_x + Q, P_{y0})$, where the DW wave number Q here appears as the period of the chain in the p_x direction.

The semiclassical solution of Eqs. (8) reads

$$G_l^{(J)} = \frac{C_l^{(J)}}{\sqrt{|v_l|}} \exp\left\{ -\frac{i}{\sigma} \int_0^{p_x} \left(p_y^{(l,J)}(p_x') - P_{y0}\right) dp_x' \right\}, \quad (9)$$

where $v_l = \partial\varepsilon/\partial p_y$ at $p_y = p_y^{(l)}(p_x)$ with indices $l = 1, 2$ denoting lower and upper trajectories. Indices $J = I, II$ denote semiclassical region, inside which the integration over p_x' is taken, that is, the left (I) and right (II) sides of the reciprocal space with respect to the MB region,i.e., to the origin defined by $p_x = 0$, as shown in Fig. 1(b). The dependence $p_y^{(l)}(p_x)$ is determined by the equality $\varepsilon(p_x, p_y) = \varepsilon$ in Eqs. (8).

These semiclassical considerations fail in narrow regions of the p-space in which semiclassical trajectories closely approach each other. Then one has to take into account the MB-quantum tunneling between the neighboring trajectories [18,19]. Dynamics of electrons in these MB regions of **p**-space is governed by the set of two equations [22,23]

$$\left[\varepsilon\left(p_x + Q/2, P_{y0} - i\sigma\frac{d}{dp_x}\right) - \varepsilon\right] G_1 + \Delta G_2 = 0,$$
$$\left[\varepsilon\left(p_x - Q/2, P_{y0} - i\sigma\frac{d}{dp_x}\right) - \varepsilon\right] G_2 + \Delta G_1 = 0, \quad (10)$$

where Δ is the amplitude of the DW order parameter introduced in Eq. (3). Note that at $H = 0$, the zeros of the determinant of this system of equations give the dispersion law of the reconstructed bands:

$$\varepsilon_\pm(p_x, p_y) = \frac{1}{2}\left[\varepsilon\left(p_x + \frac{Q}{2}, p_y\right) + \varepsilon\left(p_x - \frac{Q}{2}, p_y\right) \pm \sqrt{\left(\varepsilon\left(p_x + \frac{Q}{2}, p_y\right) - \varepsilon\left(p_x - \frac{Q}{2}, p_y\right)\right)^2 + 4\Delta^2}\right]. \quad (11)$$

To find the solution for finite magnetic fields, we note that $p_x, p_y \ll p_F$ (p_F is the Fermi momentum) in the region of the MB, and hence the dispersion functions $\varepsilon(p_x \pm Q/2, P_{y0} - i\sigma\frac{d}{dp_x})$ in the above set of equations may be expanded in both their arguments. Equations (10) can then be solved inside the MB region without using the semiclassical approximation. For magnetic fields $\hbar\omega_H \ll \varepsilon_F$, the region in which the solution of this expanded set is valid overlaps with the regions in which the semiclassical solutions Eq. (9) are valid. Matching two sets of solutions, and taking into account the above-mentioned periodic boundary condition, one finally gets the wave functions and the dispersion equation for electrons under MB conditions.

As shown in our previous papers, in both cases of the initially open [16] and closed [24] FSs, the dependence of the tunneling probability t^2 for MB between neighboring semiclassical trajectories on the DW order parameter Δ, the magnetic field H, and the Fermi energy ε_F is qualitatively different for two ranges of values of the DW momentum Q.

If Q is small, so the overlapping of the initial closed orbits is large, both velocities in the above-mentioned expansion are large ($|v_x(0,0)|, |v_y(0,0)| \sim v_F$, where $v_F = p_F/m$ is the Fermi velocity) and the tunneling probability is given by the conventional Blount formula [22,23,25],

$$t_B^2 = 1 - \exp\left\{-\frac{\Delta^2}{\hbar\omega_H m\left|v_x^{(0)} v_y^{(0)}\right|}\right\}, \quad (12)$$

where $v_x^{(0)}$ and $v_y^{(0)}$ are the velocities at the crossing points of the initial FSs.

If Q is close to $2p_F$, the initial FSs nearly touch each other, one of the above-mentioned velocities is close to zero (that is the electron system is close to the Lifshitz $2\frac{1}{2}$ transition[26]), and the tunneling probability is given by [16,24,27,28]

$$t^2 = 1 - \exp\left\{-\frac{|A|^2\Delta^2}{(\hbar\omega_H)^{4/3}(\varepsilon_F)^{2/3}}\right\},$$
$$A(\varepsilon; Q) = 2^{2/3}\pi\,\mathrm{Ai}\left[2^{2/3}\frac{\varepsilon_Q - \varepsilon}{(\hbar\omega_H)^{2/3}(\varepsilon_F)^{1/3}}\right], \quad (13)$$

where $\mathrm{Ai}(x)$ is the Airy function and $\varepsilon_Q = (Q/2)^2/2m$.

As shown in Refs. [16,24,27,28], the solution of Eqs. (10) for the case of our interest $Q \approx 2p_F$ can be presented by the integral

$$G_{1,2}(p_x) \propto \int_{-\infty}^{\infty} g_{1,2}(\xi) \exp\left\{p_x \frac{\left(2mv_x^{(0)}\right)^{1/3}}{\sigma^{2/3}}\right\} d\xi, \quad (14)$$

in which $g_{1,2}(\xi)$ is a smooth function with the characteristic interval of variation $\delta\xi \sim 1$. The wave functions $G_{1,2}(p_x)$ are of semiclassical character at $p_F \gg |p_x| \gg \sigma^{2/3}/(2mv_x^{(0)})^{1/3}$. Therefore, the regions in which the matching can be done is near $|p_x^{(\mathrm{match})}| = \sigma^{2/3}/(2mv_x^{(0)})^{1/3}$. If $|p_x^{(\mathrm{match})}| \ll \Delta/v_F$ [see Eq. (11)], one may neglect the size of the MB region in comparison to all characteristic parameters of the reconstructed spectrum. Accepting this inequality and matching the wave functions with the usage of Eqs. (13) and the periodic boundary condition, one finds the dispersion equation of electrons. Using this dispersion equation, one finally finds the density of states (DOS) [24]

$$\nu(\varepsilon) = \frac{2S'}{(2\pi\hbar)^2} \frac{|\sin(S/2\sigma)|\Theta[t^2 - \cos^2(S/2\sigma)]}{\sqrt{t^2 - \cos^2(S/2\sigma)}}. \quad (15)$$

Here $S' \equiv dS(\varepsilon)/d\varepsilon$ and $S(\varepsilon)$ is the area of the periodic chain inside one of its periods [see Fig. 1(b)]. As one can see from Eq. (15), the spectrum consists of Landau bands, of the width $\sim t^2\hbar\omega_H$, centered around the discrete Landau levels $E_n = \hbar\omega_H(n + 1/2)$, and gaps of the width $\sim(1 - t^2)\hbar\omega_H$ between them. Note that from Eqs. (13), it follows that the characteristic scale for the cyclotron frequency ω_H appears to be $(\Delta/\varepsilon_F)^{3/2}\varepsilon_F$, so the whole range of the strengths of magnetic field, including the asymptotic regimes of weak and strong magnetic fields, is physically relevant and attainable. In particular, in the limit $H \to \infty$, the MB probability $t^2 \to 0$, electrons move along closed orbits and, according to Eq. (15), $\nu(\varepsilon)$ goes to the conventional DOS of the electrons on closed orbits under quantizing magnetic field. In the opposite limit of extremely weak magnetic fields, the MB probability $t^2 \to 1$,

electrons under the magnetic field move along open trajectories [see Fig. 1(b)] and $\nu(\varepsilon)$ goes to DOS of electrons in the absence of magnetic field.

The result Eq. (15) for $\nu(\varepsilon)$ is of central importance for the considerations that follow. In particular, in the next section we calculate the electron density,

$$n(\varepsilon_F, \Delta, Q) = \int_0^{\varepsilon_F} \nu(\varepsilon) d\varepsilon, \tag{16}$$

and the electron band energy,

$$E_b(\varepsilon_F, \Delta, Q) = \int_0^{\varepsilon_F} \varepsilon \nu(\varepsilon) d\varepsilon, \tag{17}$$

at temperature $T = 0$.

IV. BAND ENERGY

Using Eq. (15), along with the change of integration variable in Eqs. (16) and (17) from ε to φ,

$$\frac{S(\varepsilon)}{2\sigma} = \varphi, \tag{18}$$

one finds the electron density and the band energy as follows:

$$n(\varepsilon_F) = \frac{4\sigma}{(2\pi\hbar)^2} \int_0^{\frac{S(\varepsilon_F)}{2\sigma}} \frac{|\sin\varphi|\Theta(t^2(\varphi) - \cos^2\varphi)}{\sqrt{t^2(\varphi) - \cos^2\varphi}} d\varphi, \tag{19}$$

$$E_b = \frac{4\sigma}{(2\pi\hbar)^2} \int_0^{\frac{S(\varepsilon_F)}{2\sigma}} \frac{\varepsilon(\varphi)|\sin\varphi|\Theta(t^2(\varphi) - \cos^2\varphi)}{\sqrt{t^2(\varphi) - \cos^2\varphi}} d\varphi, \tag{20}$$

with $\varepsilon(\varphi)$ being the solution of Eq. (18).

In Eqs. (19) and (20), ε_F is the Fermi energy of the reconstructed system under magnetic field H, which is linked to the Fermi energy $\bar{\varepsilon}_F$ of the same system at $H = 0$ by the condition of conservation of the electron number:

$$n(\varepsilon_F) = \frac{S(\bar{\varepsilon}_F)}{(2\pi\hbar)^2}. \tag{21}$$

On the other hand, $\bar{\varepsilon}_F$ is determined by the Fermi energy ε_{F0} of the initial, unreconstructed system at $H = 0$ through the condition of conservation of the number of electrons at $H = 0$,

$$S(\bar{\varepsilon}_F, Q) = S_0(\varepsilon_{F0}), \tag{22}$$

where $S_0(\varepsilon_{F0}) = \pi p_{F0}^2$ is the area of the initially closed FS [see Fig. 1(a)].

Carrying out the integration in Eq. (19) and taking into account the condition Eq. (22), one arrives at the equation that defines the new Fermi energy of the reconstructed system in magnetic field (for details, see Appendix A),

$$\cos(\pi\delta n_F) = t\cos(\pi\delta n_{F0}). \tag{23}$$

Here δn_F and δn_{F0} are the fractional parts of the ratios

$$\frac{S(\varepsilon_F)}{2\pi\sigma} = N_F + \delta n_F,$$
$$\frac{S_0(\varepsilon_{F0})}{2\pi\sigma} = N_F + \delta n_{F0}, \tag{24}$$

respectively, while N_F is the integer. Here and below we define $0 \leqslant \delta n_F, \delta n_{F0} < 1$, and hence ε_{F0} coincides with a discrete Landau level if $\delta n_{F0} = 1/2$ and it is the middle between them if $\delta n_{F0} = 0$ (the same is valid for ε_F).

Note that at extremely large magnetic fields, one has $t \to 0$, with electrons moving along closed orbits. In this limit, $\delta n_F = 1/2$ at any value of δn_{F0}, that is, the Fermi energy of free electrons under magnetic field always coincides with one of the Landau levels at any value of the filling factor.

With Eq. (19) and the condition Eq. (23) taken into account, the expression Eq. (20) for the band energy per unit area reduces (details of the calculation are given in Appendix B) to the following convenient form:

$$E_b = E_b^{(H=0)} + E_b^{(H)}. \tag{25}$$

The first term on the right-hand side of Eq. (25) is the band energy of the reconstructed system in the absence of magnetic field [6],

$$E_b^{(H=0)}(Q, \Delta) = \frac{4}{(2\pi\hbar)^2 m} \int_0^{\frac{Q}{2}} dp_x \int_0^{p_y^{(F)}} dp_y \times \left[\frac{Q^2}{2} + p_y^2 + p_x^2 - \sqrt{(Qp_x)^2 + (2m\Delta)^2}\right], \tag{26}$$

where

$$p_y^{(F)} = \left\{2m\varepsilon_F - \frac{Q^2}{2} - p_x^2 + \sqrt{(Qp_x)^2 + (2m\Delta)^2}\right\}^{\frac{1}{2}}. \tag{27}$$

Detailed analysis of this energy and conditions of the stabilization of the DW at $H = 0$ are presented in Ref. [6].

The second term in Eq. (25) is the electron "magnetic" energy, including the contribution of the MB that takes place in small regions in the vicinity of points of the closest approach of the two open trajectories:

$$E_b^{(H)} = \nu_0 \frac{(\hbar\omega_H)^2}{2} \left\{-\delta n_{F0}^2 + \frac{2}{\pi^2} \int_{\cos(\pi\delta n_{F0})}^1 \frac{\arccos(t\zeta)}{\sqrt{1-\zeta^2}} d\zeta\right\}. \tag{28}$$

Here $\nu_0 = 4\pi m/(2\pi\hbar)^2$ is the band DOS of the unreconstructed system at $H = 0$.

When the magnetic field is rather small, one has $t \approx 1$ [see Eqs. (13)],i.e., the MB is absent, and electrons move along open trajectories. As follows from Eqs. (23) and (25), the electron "magnetic" energy then tends to zero. Therefore, one has

$$E_b = E_b^{(H=0)}(Q, \Delta), \tag{29}$$

that is, the band energy and the Fermi energy [see Eq. (22)] are the same as in the absence of magnetic field.

In the other limiting case of a strong magnetic field, MB is strong ($t \to 0$), so the electrons move along closed orbits and, according to Eqs. (23) and (25), one has $\delta n_F = \frac{1}{2}$ and

$$E_b = E_b^{(H=0)}(Q, \Delta) + \nu_0 \frac{(\hbar\omega_H)^2}{2} \delta n_{F0}(1 - \delta n_{F0}). \tag{30}$$

On the other hand, taking $\Delta = 0$ in Eq. (25) one finds the band energy of the initial, unreconstructed system in the absence of the DW as follows: $\delta n_F = \frac{1}{2}$ and

$$E_b^{(\Delta=0)} = \frac{1}{2}\nu_0\varepsilon_{F0}^2 \left\{1 + \left(\frac{\hbar\omega_H}{\varepsilon_{F0}}\right)^2 \delta n_{F0}(1 - \delta n_{F0})\right\}. \tag{31}$$

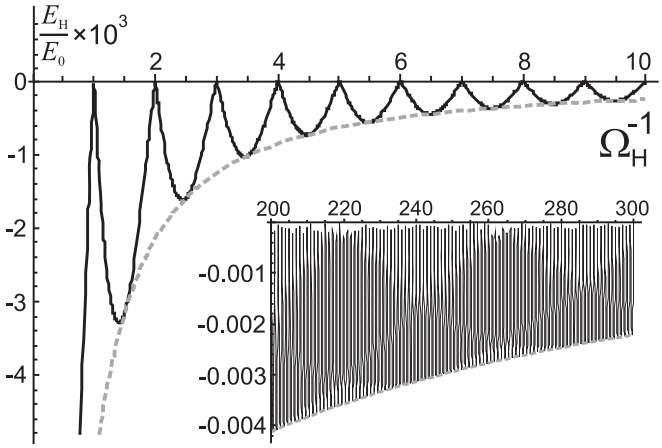

FIG. 2. De Haas-van Alphen type of oscillations of the magnetic energy gain [given by the second term in Eq. (32)], with respect to the inverse magnetic field $\Omega_H^{-1} \equiv \varepsilon_{F0}/\hbar\omega_H$. The dotted curve is the envelope showing the maximal magnetic energy gain obtained for $\delta n_{F0} = 1/2$. The inset shows the experimentally relevant interval $30T \leqslant H \leqslant 50T$, for the choice of parameters $\Delta/\varepsilon_{F0} = 0.01$, and such value of Q that maximizes t^2 in Eqs. (13).

Here $\frac{1}{2}\nu_0\varepsilon_{F0}^2$ is the initial band energy in the absence of the DW and of magnetic field. Therefore, in this limit, in both cases of reconstructed and unreconstructed systems [Eqs. (30) and (31)], the Fermi energy, ε_F, at $H \neq 0$ coincides with one of the discrete Landau levels independently of the value of the Fermi energy ε_{F0} at $H = 0$, while the band energy of electrons localized by the magnetic field (Landau electrons) is always greater than or equal to the band energy at $H = 0$.

Subtracting the initial band energy Eq. (31) from Eq. (25), one finds the decrease of the total band energy per unit area as follows:

$$\Delta E_b = \Delta E_b^{(H=0)}(Q, \Delta) + \nu_0 \frac{(\hbar\omega_H)^2}{2} \times \left\{ -\delta n_{F0} + \frac{2}{\pi^2} \int_{\cos(\pi\delta n_{F0})}^{1} \frac{\arccos(t\zeta)}{\sqrt{1-\zeta^2}} d\zeta \right\}. \quad (32)$$

The first term on the right-hand side of Eq. (32) is the energy gain of the reconstructed system with the DW in the absence of magnetic field, $H = 0$. Its Fermi energy $\bar{\varepsilon}_F$ is determined by Eq. (22). This energy was derived and analyzed in detail in our previous paper [6], in which it was proved that the DW energy is optimal if $\bar{\varepsilon}_F = \varepsilon_{F0}$. The second term is the electron magnetic energy gain which is responsible for the de Haas-van Alphen oscillations modified by MB [29]. This magnetic energy as a function of the magnetic field is shown in Fig. 2.

V. STABILITY OF THE DW ORDER

Besides the band energy Eq. (32), the complete condensation energy $E_{\rm DW}$ also includes the contribution from the periodic lattice deformation, given by the corresponding mean-field term in the Hamiltonian Eq. (3). For further analysis, more precisely for the minimization of $E_{\rm DW}$ with respect to the DW momentum Q and the order parameter Δ, it is convenient to introduce dimensionless quantities,

$$q \equiv \frac{Q}{2p_{F0}}, \quad \delta \equiv \frac{\Delta}{\varepsilon_{F0}},$$
$$\Omega_H \equiv \frac{\hbar\omega_H}{\varepsilon_{F0}}, \quad \lambda \equiv \frac{m}{\pi\hbar^2}\frac{g^2}{2\hbar\omega_Q}, \quad (33)$$

for the DW wave vector, DW order parameter, magnetic field, and coupling constant, respectively. λ is, like g, assumed to be **Q**-independent,i.e., we do not take into account the presumably smooth dependence of ω_Q on **Q** in the narrow range of values of **Q** related to the touching instability from Fig. 1. Written in terms of quantities Eqs. (33), the total condensation energy $E_{\rm DW}$, scaled by the bare band energy $E_0 = \frac{1}{2}\nu_0\varepsilon_{F0}^2$ introduced after Eq. (31), reads

$$\frac{E_{\rm DW}(\Omega_H, q, \delta)}{E_0} = \widetilde{E}_{\rm DW}^0 + \widetilde{E}_{\rm DW}^H, \quad (34)$$

where the dimensionless (scaled) partial condensation energy terms in expression Eq. (34) are

$$\widetilde{E}_{\rm DW}^0(q, \delta) = 1 - \frac{16}{3\pi}\int_0^q \left(1 - q^2 - x^2 + \sqrt{(2qx)^2 + \delta^2}\right)^{\frac{3}{2}} dx + \frac{\delta^2}{\lambda},$$
$$\widetilde{E}_{\rm DW}^H(\Omega_H, q, \delta) = \Omega_H^2 \left\{ -\delta n_{F0} + \frac{2}{\pi^2}\int_{\cos(\pi\delta n_{F0})}^{1} \frac{\arccos(|t|\zeta)}{\sqrt{1-\zeta^2}} d\zeta \right\}, \quad (35)$$

where the last term in the first expression is due to the lattice deformation.

Let us by q_m denote the optimal value of the DW wave number for which the condensation energy Eq. (34) has the minimum. To simplify its determination, we note at first that both q-dependent condensation energy contributions in Eqs. (35) have their minima at the wave numbers in the range $Q \sim 2p_F$. Let us denote these minima by q_m^0 and q_m^H, respectively. The former is explicitly given by [6]

$$q_m^0 = 1 - \frac{\delta}{2} + \frac{\delta^{3/2}}{2\sqrt{2\pi}}. \quad (36)$$

As for the latter, the minimization of $\widetilde{E}_{\rm DW}^H$ gives

$$q_m^H = \sqrt{1 + 2^{-2/3} x_m \Omega_H^{2/3}}, \quad (37)$$

where $x_m = -1.01879$ is the value that maximizes the Airy function in Eqs. (13), thus providing the equilibrium value of the tunneling probability:

$$t_m^2 = 1 - \exp\left\{ -2^{4/3}\pi^2 \mathrm{Ai}^2(x_m) \frac{\delta^2}{\Omega_H^{4/3}} \right\} = 1 - \exp\left\{ -7.14 \frac{\delta^2}{\Omega_H^{4/3}} \right\}. \quad (38)$$

Let us now approximate the expressions for $\widetilde{E}_{\rm DW}^0$ and $\widetilde{E}_{\rm DW}^H$ by the respective quadratic expansions around q_m^0 and q_m^H,

$$\widetilde{E}_{\rm DW}^{0,H}(q) \approx \widetilde{E}_{\rm DW}^{0,H}\left(q = q_m^{0,H}\right) + \tfrac{1}{2}\alpha_{0,H}\left(q - q_m^{0,H}\right)^2, \quad (39)$$

with corresponding minimal energies

$$\widetilde{E}^{0}_{\mathrm{DW}}(q^{0}_{m}) = \left(\frac{1}{\lambda} - \frac{1}{\lambda_c^{(H=0)}}\right)\delta^2 + \frac{1}{\pi}\delta^3, \tag{40}$$

$$\widetilde{E}^{H}_{\mathrm{DW}}(q^{H}_{m}) = \Omega_H^2\left\{-\delta n_{F0} + \frac{2}{\pi^2}\int_{\cos(\pi\delta n_{F0})}^{1}\frac{\arccos(t_m\zeta)}{\sqrt{1-\zeta^2}}d\zeta\right\}, \tag{41}$$

and expansion coefficients

$$\alpha_0 = \frac{16}{\pi}\left(1 - \sqrt{2} + \frac{\pi}{\sqrt{2}}\right)\delta^{\frac{1}{2}}, \tag{42}$$

$$\alpha_H = 2^{\frac{2}{3}}32x_m\mathrm{Ai}^2(x_m)\frac{\delta^2}{\Omega_H^{2/3}}\frac{1-t_m^2}{t_m^2}\ln\sqrt{\frac{1-t_m}{1+t_m}}. \tag{43}$$

The DW condensation energy in the absence of magnetic field, taken at its optimal wave vector, is given by Eq. (40) and has been elaborated in detail in Ref. [6]. There $\lambda_c^{(H=0)} = (1 + 2/\pi)^{-1} \approx 0.61$ is the critical value of the coupling constant for the DW stabilization at $H = 0$. Analogously, $\widetilde{E}^{H}_{\mathrm{DW}}(q^{H}_{m})$ in Eq. (41) is the magnetic energy taken at its own optimal wave vector q^{H}_{m}. The coefficient α_H in Eq. (43) is provided taking only the envelope of magnetic energy oscillations into account, i.e., taking $\delta n_{F0} = 1/2$ (see Fig. 2). The same manner will be used in the presentation of further results.

After inserting the expansions Eq. (39) into the expression Eq. (34), and the minimization of the latter with respect to q, one finally gets the optimal condensation energy,

$$\frac{E_{\mathrm{DW}}}{E_0} = \widetilde{E}^{0}_{\mathrm{DW}}(q^{0}_{m}) + \widetilde{E}^{H}_{\mathrm{DW}}(q^{H}_{m}) + \frac{1}{2}\frac{\alpha_0\alpha_H}{\alpha_0+\alpha_H}\left(q^{0}_{m} - q^{H}_{m}\right)^2, \tag{44}$$

and the optimal DW wave vector,

$$q_m = \frac{\alpha_0 q^{0}_{m} + \alpha_H q^{H}_{m}}{\alpha_0 + \alpha_H}. \tag{45}$$

The dependance of the DW condensation energy Eq. (44) on the order parameter and magnetic field for $q = q_m$ is shown in Fig. 3(a). It is evident that by increasing the magnetic field, the minimum of E_{DW} is lowered. This shows that magnetic field additionally strengthens stabilization of the DW.

The results of the numerical calculation of the dependence of the DW wave number q_m and of the DW amplitude δ on magnetic field for a given value of the coupling constant λ are shown in Figs. 3(b) and 3(c). q_m shows a very weak dependence on magnetic field of the order of only few percent, while the order parameter increases approximately three times within the same range of variation of magnetic field, corresponding to the span of a hundred Tesla.

The above results lead us to the phase diagram shown in Fig. 4(a). As already pointed out in the previous paper [6], in the absence of magnetic field the phase transition resulting in the DW and reconstructed electron band has the characteristics of the quantum phase transition, which takes place only providing $\lambda > \lambda_c^{(H=0)}$.

The present analysis indicates that, regarding this transition, a finite external magnetic field strengthens the DW ordering. First, as shown in Fig. 3(a), it lowers the total energy of the DW state. Second, Fig. 3(c) shows that the magnitude of

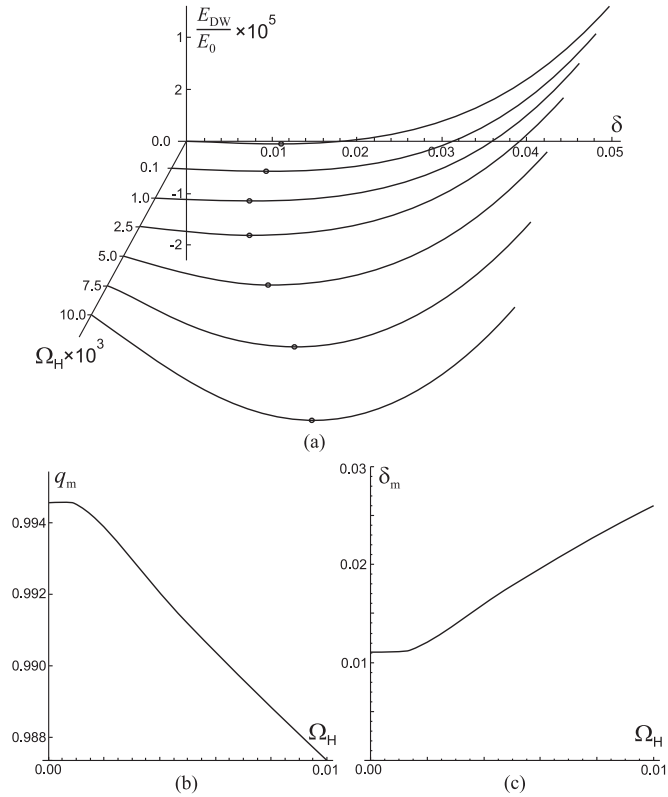

FIG. 3. (a) The dependance of the DW condensation energy Eq. (34) on the order parameter δ and the magnetic field Ω_H, taken at the optimal value of wave vector q_m and for $\lambda = 0.613$. The dependence of (b) optimal DW wave vector q_m, and of (c) optimal DW order parameter δ_m, on Ω_H, for the same value of λ.

the order parameter δ increases as H increases. Furthermore, by switching the external magnetic field, one introduces a qualitative change into the DW phase diagram. Namely, as Fig. 4(a) shows, the domain of values of parameters Ω_H and λ for which the DW is stable extends toward lower and lower values of the coupling constant λ as Ω_H increases. Only, below the critical curve $\lambda_c(\Omega_H)$, the ordering is suppressed, i.e., the order parameter δ vanishes within the range

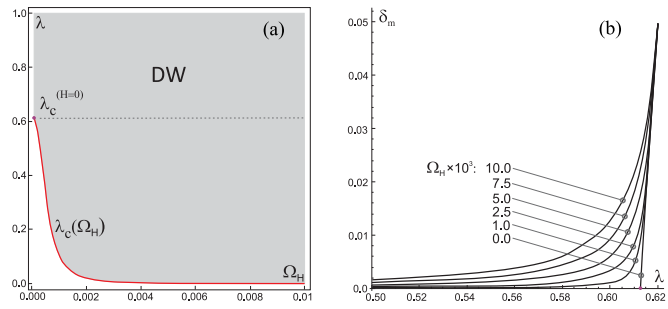

FIG. 4. Phase diagram: (a) The DW is present in the shaded domain of the (Ω_H, λ) plane, with the curve $\lambda_c(\Omega_H)$ representing the critical value of the coupling constant below which the DW order parameter vanishes. The dashed line at $\lambda = \lambda_c^{H=0}$ is the critical line below which the DW order is possible only in finite magnetic field. (b) DW order parameter δ_m vs λ for a series of values of Ω_H.

of numerical imprecision. We see that such effective critical coupling $\lambda_c(\Omega_H)$ saturates to zero at a finite value of H, roughly estimated to be of the order of a few dozen Tesla. In other words, there is a range of values of the coupling constant in which the DW order and the band reconstruction, although not possible at $H = 0$, can be induced by applying the external magnetic field. In Fig. 4(b), we show the equilibrium value of the DW order parameter δ_m vs λ for a series of different values of magnetic field Ω_H.

VI. CONCLUSION

The results presented above show that a strong enough external magnetic field strengthens the tendency of an isotropic 2D electron band toward the band reconstruction, associated with the formation of uniaxial DW that breaks the translational symmetry of the system. The band reconstruction under magnetic field is the result of two opposing tendencies. From one side, in the magnetic field, open 1D trajectories are additionally energetically favored with respect to the closed Landau quantized orbits in the initial unreconstructed 2D band. From the other side, the closeness of oppositely directed open trajectories from Fig. 1 inevitably provokes a MB between them. Finite tunneling probability between these trajectories causes a partial relocalization of band states and thus acts against the DW stability.

In the above analysis, we use the well-established semiclassical approach of electron dynamics in the magnetic field, together with the full quantum mechanical treatment of the MB. The obtained band spectrum consists of an alternating sequence of narrow energy subbands and energy subgaps [19], each subband being located around a Landau discrete level.

The knowledge of the associated DOS Eq. (15) opened the way toward the calculation of the total condensation energy at zero temperature, given by Eq. (34). The important outcome of this calculation is the additivity of the band energy gain. It has two contributions, one due to the bare $H = 0$ band reconstruction, and another due to the above-mentioned effects of finite magnetic field. The former comes from redistribution of the DOS toward lower energies in the reconstructed band [6]. The latter comes, as already stated above, from the delocalization of initially Landau-localized electrons, modified by the MB. It is accompanied by quantum oscillations periodic in $1/H$, similar to the standard de Haas-van Alphen effect, due to Landau-level filling (see Fig. 2).

The next important element which facilitates the further minimization of the condensation energy Eq. (34) is the closeness of values of optimal wave numbers which minimize these two contributions. Both are close to $2p_F/\hbar$ (see Fig. 1), differing only by a few percent. The final optimal DW wave number, minimizing the total condensation energy, is an adequate mean of these two, given by Eq. (45) and shown in Fig. 3.

The central result of the whole analysis is the phase diagram shown in Fig. 4, from which one concludes that the external magnetic field strengthens the DW quantum phase transition with respect to that stabilized at $H = 0$. One measure of this strengthening is the increase of the order parameter by approximately three times along the span of magnetic field up to a hundred Tesla. Simultaneously, the optimal wave number decreases only by a few percent in the same domain, the reasons for this weak variation being already pointed out above. Finally, the critical value of the coupling constant λ, beyond which quantum phase transition takes place, decreases by increasing H, and quickly saturates toward zero at the field domain of a few dozen Tesla. The external magnetic field thus opens possibility for DW and band reconstruction to appear in materials in which they are not present in zero field.

ACKNOWLEDGMENTS

This work was supported by the Croatian Science Foundation, Project No. IP-2016-06-2289, and by the QuantiXLie Centre of Excellence, a project cofinanced by the Croatian Government and European Union through the European Regional Development Fund—the Competitiveness and Cohesion Operational Programme (Grant No. KK.01.1.1.01.0004).

APPENDIX A: CALCULATIONS OF THE ELECTRON NUMBER

As $S(\varepsilon_F)/2\sigma = \varepsilon_F/\hbar\omega_H \gg 1$, it is convenient to rewrite the upper integration limit of the first integral in Eq. (19) in the form $\pi(N_F + \delta n_F)$ (where N_F and $0 \leqslant \delta n_F < 1$ are the integer and fractional parts of $S(\varepsilon_F)/2\sigma$, respectively, and present the integral as a sum of integrals over two intervals, $(l\pi, (l+1)\pi)$ and $(0 \leqslant l \leqslant N_F - 1)$. After the change of variables $\varphi - l\pi \to \varphi$, one finds

$$n = \frac{4\sigma}{(2\pi\hbar)^2} \sum_{l=0}^{N_F-1} \int_0^{\pi} \frac{|\sin\varphi|\Theta\left(t_l^2 - \cos^2\varphi\right)}{\sqrt{t_l^2 - \cos^2\varphi}} d\varphi + \int_0^{\pi\delta n_F} \frac{|\sin\varphi|\Theta(t^2 - \cos^2\varphi)}{\sqrt{t^2 - \cos^2\varphi}} d\varphi, \tag{A1}$$

where $t_l = t(\varphi + l\pi)$ and $t = t(\varphi + (N_F - 1)\pi) \approx t(\varepsilon_F)$.

As one sees from Eqs. (12) and (13), the characteristic variation interval of $t(\varphi)$ is $\delta\varphi \sim (\varepsilon_F/\hbar\omega_H)^{1/3}\pi \gg \pi$, and hence t_l and t may be considered as constants inside each interval of the integrations with high accuracy. Under the latter condition, the integrals under the sum in Eq. (A1) are table integrals equal to π, and hence the electron density reads

$$n = \left[\pi N_F + \int_{\cos\frac{\pi\delta n_F}{t}}^{1} \frac{\Theta(1-\xi^2)}{\sqrt{1-\xi^2}} d\xi\right]. \tag{A2}$$

While writing the above equation, we changed the variable in the last integral in Eq. (A1): $\cos\varphi = t\xi$.

Inserting this result into the electron number conservation law given by Eqs. (21) and (22), one gets the equation that couples the Fermi energy of the metal with DW and the initial Fermi energy ε_{F0} at $H = 0$:

$$\pi\delta n_{F_0} = \int_{\cos\frac{\pi\delta n_F}{t}}^{1} \frac{\Theta(1-\xi^2)}{\sqrt{1-\xi^2}} d\xi. \tag{A3}$$

Here δn_{F0} is the fractional part of $S(\varepsilon_{F0})/2\sigma$. As $\delta n_F < 1$ by definition, the only solution of this equation is Eq. (23) of the main text.

APPENDIX B: CALCULATIONS OF THE BAND ENERGY

After presenting the integral in Eq. (20) as a sum of integrals over intervals $(l\pi, (l+1)\pi)$ and $(0 \leqslant l \leqslant N_F - 1)$, and changing the variables $\varphi - l\pi \to \varphi$ in the same way as in Appendix A, the band energy reads

$$E_b^{(H)} = E_b^{(1)} + E_b^{(2)}, \tag{B1}$$

where

$$E_b^{(1)} = \frac{4\sigma}{(2\pi\hbar)^2}\int_0^{\pi\delta n_F} \varepsilon(\pi N_F + \varphi)B[\varphi; t(\varepsilon_F)]d\varphi \tag{B2}$$

and

$$E_b^{(2)} = \frac{4\sigma}{(2\pi\hbar)^2}\int_0^{\pi} d\varphi \sum_{l=0}^{N_F-1} \varepsilon(\pi l + \varphi)B[\phi; t(\varepsilon(l\pi + \varphi))]. \tag{B3}$$

Here

$$B[\varphi; t(\varepsilon(\varphi))] = \frac{|\sin\varphi|\Theta[t[\varepsilon(\varphi)]^2 - \cos^2\varphi]}{\sqrt{t[\varepsilon(\varphi)]^2 - \cos^2\varphi}}. \tag{B4}$$

1. Calculations of the integral in Eq. (B2)

The dependence of energy on φ in Eq. (B2) is determined by the equation

$$\frac{S(\varepsilon)}{2\sigma} = \pi N_F + \varphi. \tag{B5}$$

As the integration here goes in the vicinity of the Fermi energy in the range $\lesssim \hbar\omega_H$, it is convenient to expand the area here as $S(\varepsilon) \approx S(\bar{\varepsilon}_F) + \delta\varepsilon S'(\bar{\varepsilon}_F)$, where $\delta\varepsilon = \varepsilon - \bar{\varepsilon}_F$.

According to Ref. [6]:

$$S(\varepsilon) = 4\int_0^{Q/2} \sqrt{2m\varepsilon - \frac{Q^2}{2} - p_x^2 + \sqrt{(Qp_x)^2 + (2m\Delta)^2}}. \tag{B6}$$

Taking the derivative with respect to ε and changing variables $p_x = p_F\xi$, one finds

$$S(\varepsilon) = S(\varepsilon_F) + 4m\delta\varepsilon\int_0^1 \frac{d\xi}{\sqrt{\delta - q^2 - \xi^2 + \sqrt{4\xi^2 + \delta^2}}}, \tag{B7}$$

where $\delta = \Delta/\varepsilon_F$ and q in the last term is taken equal to $q = p_F(1 - \delta/2)$, which presents the optimal DW vector in the lowest approximation in δ, $\hbar\omega_H/\varepsilon_F \ll 1$.

Changing variables $\zeta^2 = 4\xi^2 + \delta^2$ and performing integration, one finds the needed expansion as follows:

$$S(\varepsilon) = S(\bar{\varepsilon}_F) + 2\pi m(\varepsilon - \bar{\varepsilon}_F). \tag{B8}$$

Rewriting Eq. (B5) as $S((\varepsilon) = 2\sigma[\pi(N_F + \delta\bar{n}_F) - \pi\delta\bar{n}_F + \varphi] = S(\bar{\varepsilon}_F) + 2\sigma(\varphi - \pi\delta\bar{n}_F)$ with the usage of Eq. (B6), one finds

$$\varepsilon(\varphi + \pi N_F) = \bar{\varepsilon}_F + \frac{\sigma}{\pi m}(\varphi - \pi\delta\bar{n}_F), \tag{B9}$$

where $\delta\bar{n}_F$ is the fractional part of the ratio

$$\frac{S(\bar{\varepsilon}_F)}{2\pi\sigma} = N_F + \delta\bar{n}_F, \tag{B10}$$

while N_F is integer. Note that according to Eq. (22), one has $\delta\bar{n}_F = \delta n_{F0}$.

Inserting the above equation into Eq. (B2), and performing the integration with respect to φ, one finds

$$E_b^{(1)} = \frac{\sigma}{(2\pi\hbar)^2}\left\{\pi\bar{\varepsilon}_F\delta\bar{n}_F + \frac{\sigma}{\pi m}\left[\int_{\cos(\pi\delta\bar{n}_F)}^1 \frac{\arccos(t\zeta)}{\sqrt{1-\zeta^2}}d\zeta - (\pi\delta\bar{n}_F)^2\right]\right\}. \tag{B11}$$

2. Calculations of $E_b^{(2)}$

The sum in Eq. (B3),

$$A = \sum_{l=0}^{N_F-1} \varepsilon(\pi l + \varphi)B[\varphi; t(\varepsilon(l\pi + \varphi))], \tag{B12}$$

may be presented as follows:

$$A = \frac{1}{\pi}\sum_{k=-\infty}^{\infty}\int_{-\pi/2}^{(N_F-1/2)\pi} dx\exp\{i2kx - 2|k|\eta\} \times \varepsilon(x+\varphi)B[\varphi; t(\varepsilon(x+\varphi))]. \tag{B13}$$

While writing this equation, we used the equality

$$\sum_{l=-\infty}^{\infty}\delta[x - l\pi] = \frac{1}{\pi}\sum_{k=-\infty}^{\infty}\exp\{i2kx - 2|k|\eta\}, \tag{B14}$$

where $\eta \to 0$.

Changing the integration variables,

$$\frac{S(\varepsilon)}{2\sigma} = x + \varphi, \tag{B15}$$

one finds

$$A = \frac{1}{2\pi\sigma}\int_{\varepsilon_1}^{\varepsilon_2}\varepsilon S'(\varepsilon)B[\varphi; t(\varepsilon)]d\varepsilon + \sum_{k=1}^{\infty}\exp\{-2k\eta\} \times \int_{\varepsilon_1}^{\varepsilon_2}\varepsilon S'(\varepsilon)B[\varphi; t(\varepsilon)]\left(e^{i2k(\frac{S(\varepsilon)}{2\sigma} - \varphi)} + \text{c.c.}\right), \tag{B16}$$

where $\varepsilon_{1,2}$ are defined by the equations

$$\frac{S(\varepsilon_1)}{2\sigma} = -\frac{\pi}{2} + \varphi, \quad \frac{S(\varepsilon_2)}{2\sigma} = \left(N_F - \frac{1}{2}\right)\pi + \varphi. \tag{B17}$$

The main contributions to the integrals under the summation on the right-hand side of the above equation come from the ends of integration interval ε_1 and ε_2 because $S/2\sigma \gg 1$, and the exponents there are fast oscillating functions, while $S' \neq 0$ (hence there is no saddle point). Expanding the functions in the integrand in the vicinity of the ending points $\varepsilon_{1,2}$ and carrying out the integration, one finds that the integral under the summation sign is equal to zero at any $k \neq 0$, and hence the first term on the right-hand side of Eq. (B16) only remains. Inserting it into Eq. (B3), one finds the first term on

the right-hand side of the band energy as follows:

$$E_b^{(2)} = \frac{2}{(2\pi\hbar)^2\pi}\int_0^{\pi} d\varphi \int_{\varepsilon_1}^{\varepsilon_2} d\varepsilon\varepsilon S'(\varepsilon)B[\varphi;t(\varepsilon)]. \quad \text{(B18)}$$

Further on, changing variables in the integral with respect to the energy

$$\frac{S(\varepsilon)}{2\sigma} = \varphi_1 + \varphi - \frac{\pi}{2}, \quad \text{(B19)}$$

one finds

$$E_b^{(2)} = \frac{4\sigma}{(2\pi\hbar)^2\pi}\int_0^{\pi} d\varphi \int_0^{\pi N_F} d\varphi_1 \varepsilon\left(\varphi_1 + \varphi - \frac{\pi}{2}\right) \times B[\varphi; t(\varepsilon(\varphi_1 + \varphi - \pi/2))]. \quad \text{(B20)}$$

As the integration with respect to φ is inside the interval $(0, \pi)$, one may expand the area [as was done in Eqs. (B6) and (B9)], and find

$$\varepsilon\left(\varphi_1 + \varphi - \frac{\pi}{2}\right) = \varepsilon(\varphi_1) + \frac{2\sigma}{m}\left(\varphi - \frac{\pi}{2}\right). \quad \text{(B21)}$$

Inserting this expansion in the above integral and performing integration with respect to φ, after simple but rather lengthy calculations, one finds

$$E_b^{(2)} = \int_0^{\bar{\varepsilon}_F} \varepsilon\nu(\varepsilon)d\varepsilon + \frac{4\sigma}{(2\pi\hbar)^2} \times \left\{ -\pi\bar{\varepsilon}_F\delta n_{F0} + \frac{\hbar\omega_H}{2\pi}(\pi\delta n_{F0})^2 \right\}. \quad \text{(B22)}$$

While writing the above equation, we used the equality $\delta\bar{n}_F = \delta n_{F0}$ [see Eq. (B10) and the text below it].

Inserting Eqs. (B11) and (B22) in Eq. (B1), one obtains the band energy of the system with DW under magnetic fields, Eq. (25) of the main text.

[1] G. Grüner, *Density Waves in Solids* (Perseus Publishing, Cambridge, MA, 1994).
[2] R. E. Peierls, Ann. Phys. **4**, 121 (1930).
[3] J. P. Pouget, Semicond. Semimet. **27**, 87 (1988); Crystals **2**, 466 (2012).
[4] B. Keimer, S. A. Kivelson, M. R. Norman, S. Uchida, and J. Zaanen, Nature **518**, 179 (2015).
[5] K. C. Rahnejat, C. A. Howard, N. E. Shuttleworth, S. R. Schofield, K. Iwaya, C. F. Hirjibehedin, C. Renner, G. Aeppli, and M. Ellerby, Nat. Commun. **2**, 558 (2011); R. Shimizu, K. Sugawara, K. Kanetani, K. Iwaya, T. Sato, T. Takahashi, and T. Hitosugi, Phys. Rev. Lett. **114**, 146103 (2015).
[6] A. M. Kadigrobov, A. Bjeliš, and D. Radić, Phys. Rev. B **97**, 235439 (2018).
[7] T. Wu, H. Mayaffre, S. Krämer, M. Horvatić, C. Berthier, W. N. Hardy, R. Liang, D. A. Bonn, and M. H. Julien, Nature **477**, 191 (2011).
[8] F. Laliberté, J. Chang, N. Doiron-Leyraud, E. Hassinger, R. Daou, M. Rondeau, B. J. Ramshaw, R. Liang, D. A. Bonn, W. N. Hardy, S. Pyon, T. Takayama, H. Takagi, I. Sheikin, L. Malone, C. Proust, K. Behnia, and L. Taillefer, Nat. Commun. **2**, 432 (2011).
[9] D. LeBoeuf, N. Doiron-Leyraud, J. Levallois, R. Daou, J.-B. Bonnemaison, N. E. Hussey, L. Balicas, B. J. Ramshaw, Ruixing Liang, D. A. Bonn, W. N. Hardy, S. Adachi, C. Proust, and L. Taillefer, Nat. Lett. **450**, 533 (2007).
[10] L. P. Gor'kov and A. G. Lebed, J. Phys. Lett. **45**, 433 (1984).
[11] M. Héritier, G. Montambaux, and P. Lederer, J. Phys. C **19**, L293 (1986).
[12] D. Radić, A. Bjeliš, and D. Zanchi, Phys. Rev. B **69**, 014411 (2004).
[13] L. P. Gor'kov and A. G. Lebed, Phys. Rev. B **51**, 3285 (1995).
[14] D. Radić, A. Bjeliš, and D. Zanchi, J. Phys. IV France **114**, 129 (2004).
[15] A. M. Kadigrobov, A. Bjeliš, and D. Radić, Phys. Rev. Lett. **100**, 206402 (2008).
[16] A. M. Kadigrobov, A. Bjeliš, and D. Radić, Eur. Phys. J. B **86**, 276 (2013).
[17] Magnetic-field-induced DW in conductors with open FS in the absence of the magnetic breakdown was considered by A. G. Lebed, Phys. Rev. Lett. **88**, 177001 (2002).
[18] M. H. Cohen and L. M. Falicov, Phys. Rev. Lett. **7**, 231 (1961).
[19] M. I. Kaganov and A. A. Slutskin, Phys. Rep. **98**, 189 (1983).
[20] I. M. Lifshitz and A. M. Kosevich, Sov. Phys. JETP **2**, 636 (1955).
[21] L. Onsager, Philos. Mag. **43**, 1006 (1952).
[22] A. A. Slutskin, Zh. Eksp. Teor. Fiz. **53**, 767 (1967) [Sov. Phys.-JETP **26**, 474 (1968)].
[23] A. A. Slutskin and A. M. Kadigrobov, Fiz. Tverd. Tela (Leningrad) **9**, 184 (1967) [Sov. Phys.- Solid State **9**, 138 (1967)].
[24] A. M. Kadigrobov, D. Radić, and A. Bjeliš, Physica B **480**, 248 (2015).
[25] E. I. Blount, Phys. Rev. **126**, 1636 (1962).
[26] I. M. Lifshitz, Zh. Eksp. Teor. Fiz. **38**, 1569 (1960) [Sov. Phys.-JETP **11**, 1130 (1960)].
[27] A. M. Kadigrobov, A. A. Slutskin, and S. A. Vorontsov, J. Phys. Chem. Solids **53**, 387 (1992).
[28] J.-Y. Fortin and A. Audouard, Low Temp. Phys. **43**, 173 (2017).
[29] Note that the band reconstruction within the presently analyzed model generates two open semicircular Fermi curves (with the exception of narrow touching ranges), as shown in Fig. 1. Unlike the case of almost perfect sinusoids that characterize the band geometry of quasi-1D Bechgaard salts, these curves are badly nested. For this reason, one cannot stabilize the cascade of field-induced DW subphases with quantizied wave numbers [see, e.g., G. Montambaux, M. Héritier, and P. Lederer, Phys. Rev. Lett. **55**, 2078 (1985)], observed in some Bechaard salts.